Electronic Supplementary Information (ESI)

MOF-derived Co$_{1.11}$Te$_2$ with half-metallic characteristic for efficient photochemical conversion of CO$_2$ under visible-light irradiation

Yong Xu,[ab] Jiang Mo,[a] Guanqun Xie,[a] Dawei Ding,[b] Shujiang Ding,[b] Xiaoxia Wang*[a] and Chen Li*[a]

[a]*School of Environment and Civil Engineering, Dongguan University of Technology, Dongguan, 523808, P.R. China*

[b]*Department of Applied Chemistry, School of Science, Xi´an Jiaotong University, Xi´an, 710049, P.R. China*

*Corresponding Author
E-mail: X. Wang, wangxx@dgut.edu.cn; C. Li, lichen@dgut.edu.cn

Experimental section

Synthesis of cubic ZIF-67

In a typical procedure,[1] 291 mg of $Co(NO_3)_2 \cdot 6H_2O$ and 4.5 mg of CTAB were added into 10 mL of deionized water, then the mixture was stirred at room temperature for 10 min. The resulting solution was rapidly injected into 70 mL of aqueous solution with 4.54 g of 2-methylimidazole. After being stirred vigorously for 20 min, the mixed solution was kept still until next day. The purple precipitate was collected and washed with ethanol three times before vacuum drying at 50 °C overnight.

Preparation of $Co_{1.11}Te_2 \subset C$

200 mg of synthesized c-ZIF-67 and 500 mg Te powder were placed at two separated positions in an alumina boat with ZIF-67 nanocubes at the downstream side. The samples were heated to 700 °C with the heating rate of 10 °C min^{-1}, and maintained for 3 hours under Ar atmosphere. After cooling to room temperature naturally, the $Co_{1.11}Te_2 \subset C$ was acquired. For $CoTe_2 \subset C$, 400 mg of Te powder was placed at the upstream side, and the furnace tube was heated to 670 °C, while other conditions remained unchanged.

Characterization

The obtained materials were characterized by powder X-ray diffraction on a Japan Rigaku Ultima-IV multipurpose X-ray diffractometer with Cu K_α (λ =1.54178 Å) to identify their phases. The morphology and lattice fringes of the samples were analyzed on a thermal field emission scanning electron microscope (Hitachi SU-70) and transmission electron microscope (JEM 2100F) with an accelerating voltage of 200 kV. The STEM and EDX elemental mappings were taken on field emission transmission electron microscope (FEI Tecnai G2 F20). The produced CO and H_2 were measured by gas chromatograph (GC-2014C, Shimadzu, with argon as a carrier gas) with a 5 Å molecular sieve column (3 m × 2 m) and a thermal-conductivity detector. The liquid phase of the reaction system was determined by ^1H nuclear magnetic resonance spectroscopy (BrukerAvance 400 spectrometer) and liquid chromatogram (Agilent

1260). The product of $^{13}CO_2$ isotopic experiment was analyze by gas mass spectrometry analyzer (Pfeiffer OmniStarTM). Element analysis data of samples were obtained using inductively coupled plasma-optical emission spectrometer (Perkin Emimer Optimal-8000) and elemental analyzer (Vario EL III). Specific surface area was estimated from the amount of N_2 adsorped by using Brunaure-Emmett-Teller equilibrium equation at 77 K and recorded on an ASAP 2020. Raman spectroscopy was performed on a France Horiba LabRAM HR800 micro-Raman spectrometer using 532 nm excitation laser. X-ray photoelectron spectroscopy was carried out on a PHI 5300 ESCA using an Al K_α X-ray source with a power of 250 W. The charge effect was calibrated using the binding energy of C1s.

Photocatalytic test

Typically, 5 mg photosensitizer [Ru(bpy)$_3$]Cl$_2$·6H$_2$O and 1 mg catalyst were dispersed in a solution of acetonitrile/TEOA/H$_2$O (4 mL/1.5 mL/1 mL) using an 55 mL quartz tube. The suspension was purged with CO_2 to drive away the air, and then the tube was filled with CO_2 to conduct the reaction. During the potocatalytic reduction, the sealed tube was irradiated with a 200 W white LEDs lamp under stirring. After the reaction, the produced gases were analyzed and quantified by gas chromatograph.

To evaluate the durability of the sample, the partition strategy was employed to compensate for filtration and transferred loss of Co$_{1.11}$Te$_2$⊂C among the cycles. In each cycle, 1 mg of Co$_{1.11}$Te$_2$⊂C was taken out from a total of 6 mg for photoreaction, then after each 1 mg cycle, the parallel experiment was carried out for the rest of catalyst under the same conditions. Subsequently, all the catalysts were collected together, after washing and drying, another 1 mg of catalyst was taken out for the following run. The selectivity of CO was calculated using the equation below, mol(gas) is the molar quantity of produced gas, which is obtained from the calculation of the peak area.

$$\text{Selectivity of CO} = \text{mol(CO)}/[\text{mol(CO)} + \text{mol(H}_2)] \times 100\%$$

Computational Details

First-principles density functional theory (DFT) calculations were performed using the projected augmented wave (PAW).[2] The Perdew-Burke-Ernzerhof exchange-

correlation functional of the generalized-gradient approximation (PBE-GGA+U) was adopted for the exchange-correlation functional.[3] In all calculations, the plane-wave expansion of the wave functions with an energy cutoff of 400 eV was applied. During the relaxation, the force tolerance was set to 0.05eV/Å.

The CO_2 photoreduction pathways for the atomic layers may be proposed as following:

$$* + CO_2 \rightarrow CO_2*$$
$$CO_2* + H^+ + e^- \rightarrow COOH*$$
$$COOH* + H^+ + e^- \rightarrow CO* + H_2O$$
$$CO* \rightarrow * + CO\uparrow$$
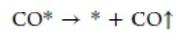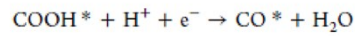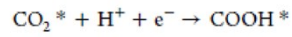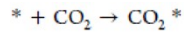
To achieve deeper insight into the reaction process, DFT calculations were further implemented on these possible reaction steps. The CO_2 photoreduction process was initiated with proton-coupled electron transfer to the adsorbed CO_2 molecules to produce the COOH* intermediate, and the subsequent protonation of COOH* led to the formation of CO*, which would finally desorb from the surface of atomic layers to generate free CO molecules. As shown in Figure, the COOH* formation process could be regarded as the rate-determining step for $CoTe_2$, in which the barrier energy of 1.06 eV was relatively mild for the CO_2 photoreduction. Meanwhile, CO* formation was an exothermic process (-1.13 eV), which could occur spontaneously. Finally the desorption energy of CO molecules was 0.7 eV, which indicated the process also need to absorb energy. For $Co_{1.11}Te_2$, the COOH* formation process is easier than $CoTe_2$ with the barrier energy of 0.093 eV, which make $Co_{1.11}Te_2$ more efficient for CO_2 photoreduction.

The generalized gradient approximation (GGA) with the Perdew-BurkeErnzerhof exchange-correlation functional[3] and a 400-eV cutoff for the plane-wave basis set are employed to perform all the density functional theory (DFT) computations within the frame of Vienna *ab initio* simulation package (VASP).[4,5] The projector-augmented plane wave (PAW) is used to describe the electron-ion interactions.[6,7] The 4*2*1 *k*-point mesh is employed for geometric optimization. The convergence threshold is set as 10^{-6} eV in energy and 0.05 eV/Å in force. For all the calculations of slab models, the

symmetrization is switched off.
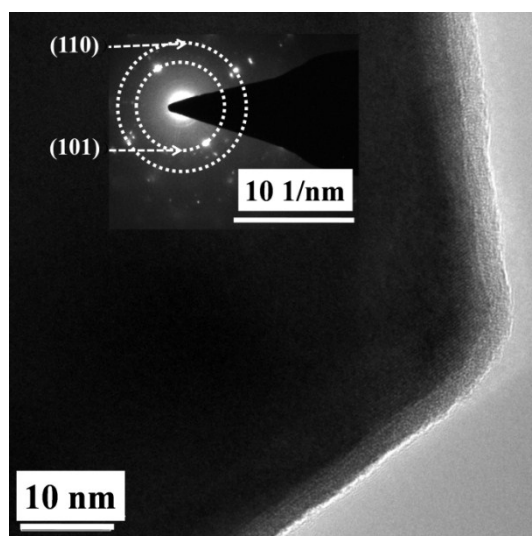
Fig. S1. TEM image of $Co_{1.11}Te_2 \subset C$. Inset is the SAED pattern.
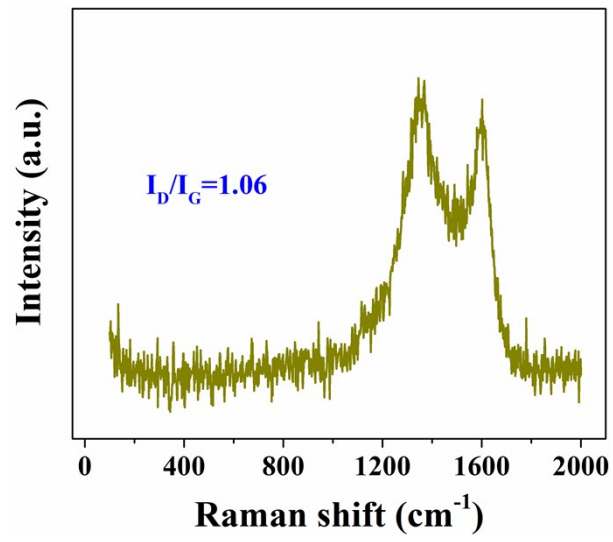
Fig. S2. Raman spectrum of $Co_{1.11}Te_2 \subset C$ sample.
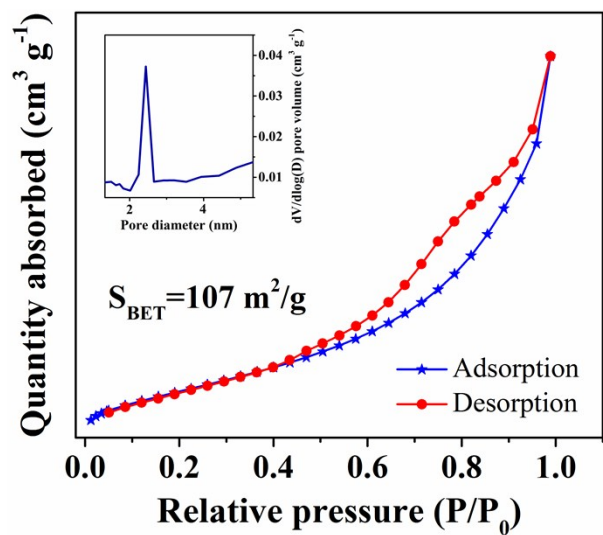
Fig. S3. N_2 adsorption-desorption isotherms and the corresponding pore size distribution (inset) of $Co_{1.11}Te_2 \subset C$.
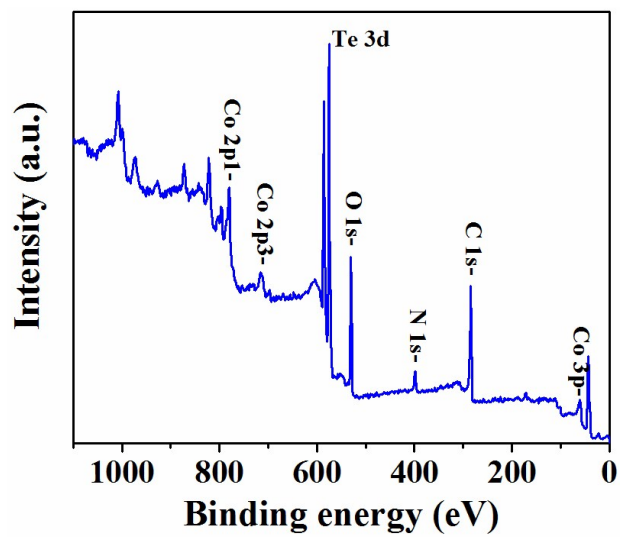
Fig. S4. Survey-scan XPS spectrum of $Co_{1.11}Te_2 \subset C$.
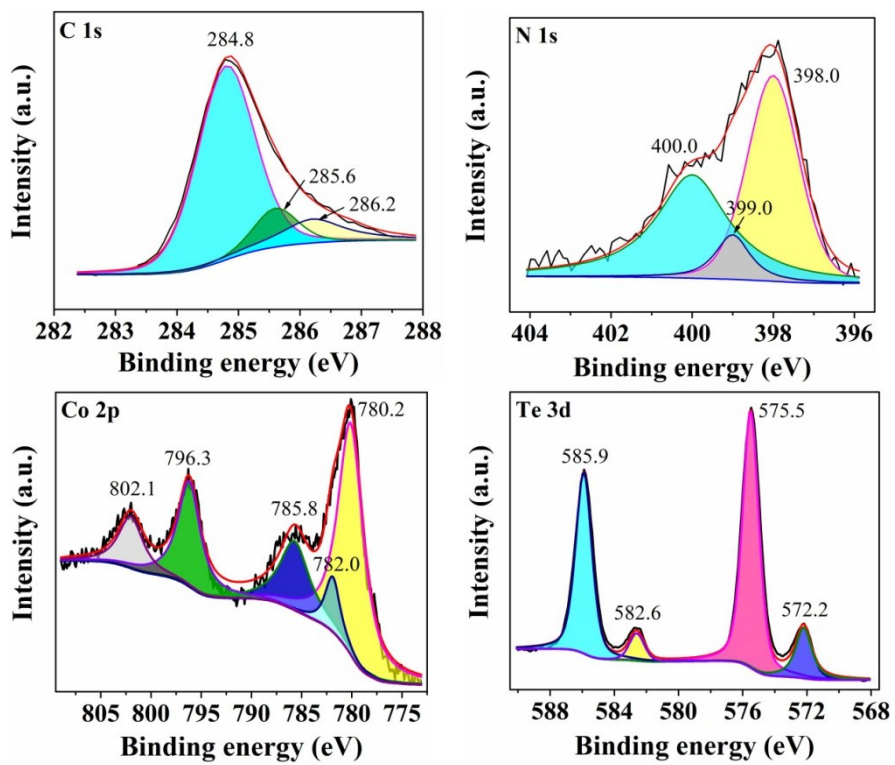
Fig. S5. High-resolution XPS spectra of C 1s, N 1s, Co 2p and Te 3d.
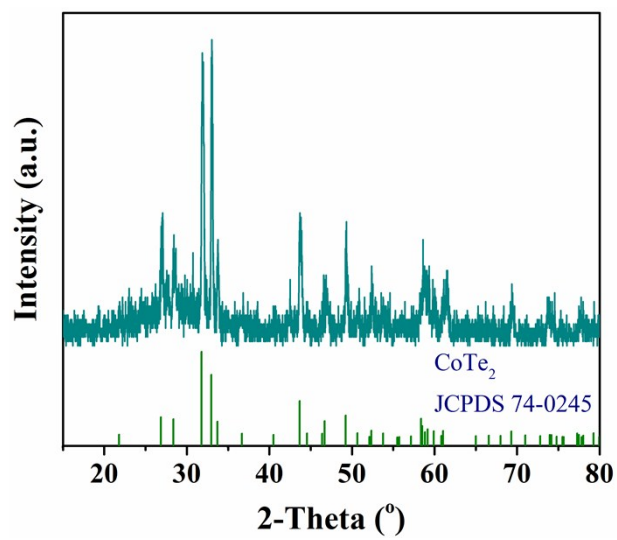
Fig. S6. XRD pattern of $CoTe_2 \subset C$.
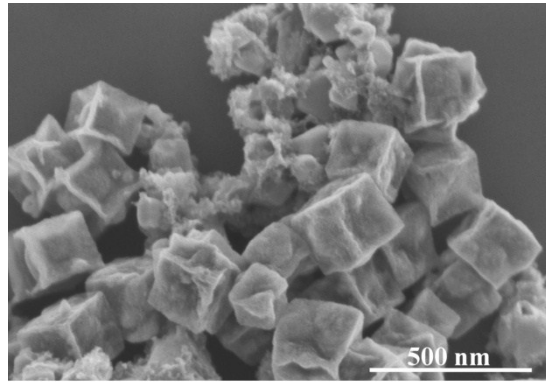
Fig. S7. SEM image of CoTe$_2$⊂C.
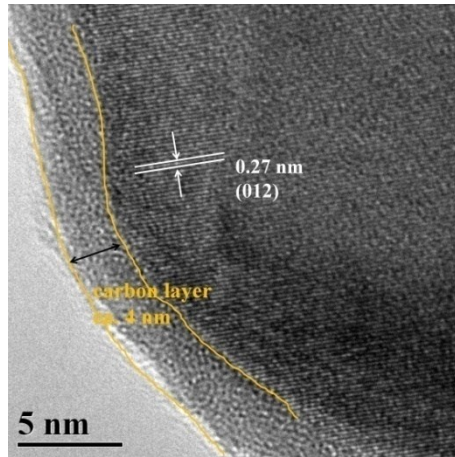
Fig. S8. TEM image of CoTe$_2$⊂C.
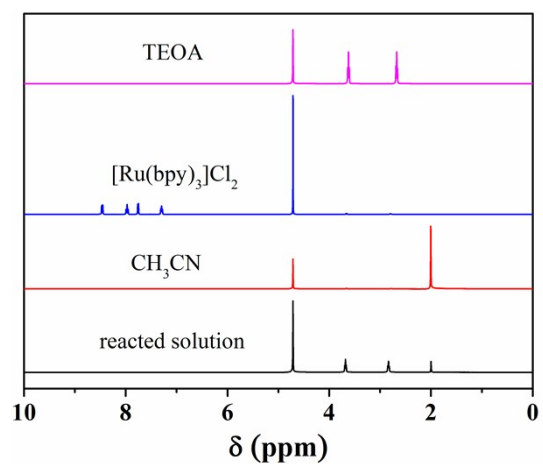
Fig. S9. ^{1}H NMR of the reaction solution after irradiation.
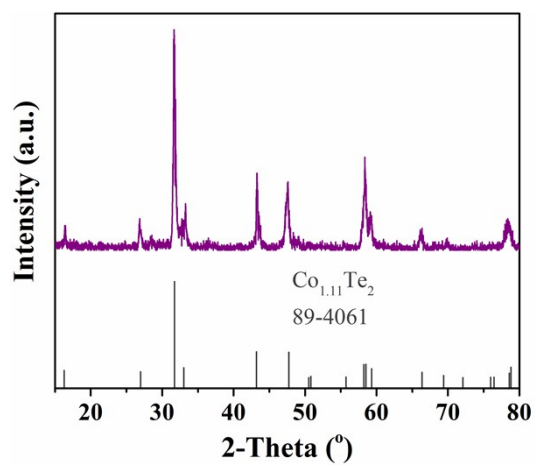
Fig. S10. XRD pattern of recycling $Co_{1.11}Te_2 \subset C$.
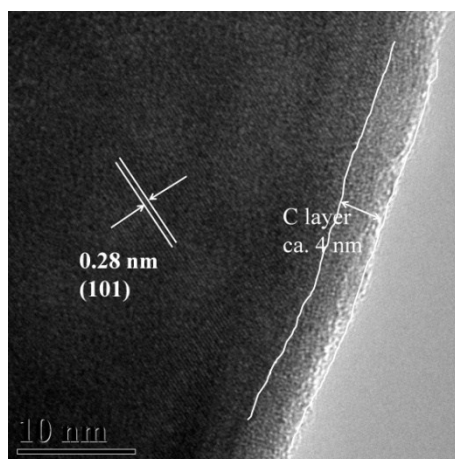
Fig. S11. TEM image of recycling $Co_{1.11}Te_2 \subset C$.
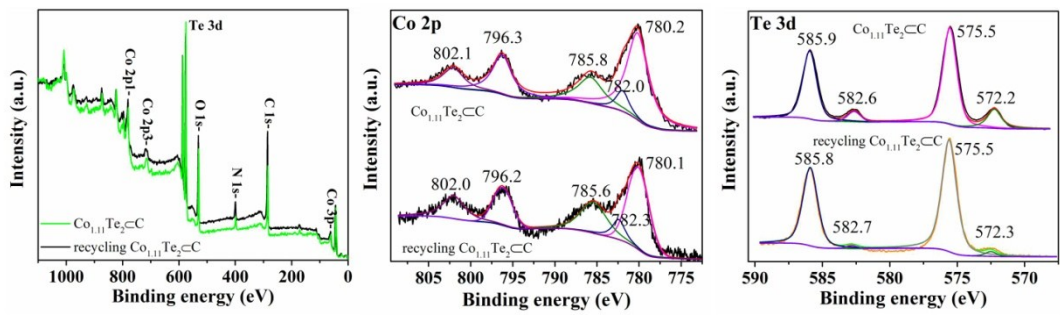
Fig. S12. The comparison of XPS spectra between $Co_{1.11}Te_2 \subset C$ and recycling $Co_{1.11}Te_2 \subset C$.

Table S1. Element contents of $Co_{1.11}Te_2 \subset C$.

Element	Co	Te	C	N
Content (wt%)	16.11	62.87	19.90	1.12
Atomic ratio	1.11	2.01	6.73	0.32

Table S2. Control experiments of photocatalytic CO_2 reduction.[a]

Entry	Catalyst/ $Co_{1.11}Te_2 \subset C$	Photosensitizer/ $[Ru(bpy)_3]Cl_2 \cdot 6H_2O$	CO_2	TEOA	Light	Yield of CO (μmol)	Yield of H_2 (μmol)
1	×	√	√	√	√	0	1.5
2	√	×	√	√	√	0	0
3[b]	√	√	×	√	√	0	12.6
4	√	√	√	×	√	0	0
5	√	√	√	√	×	0	0.6
6	√	√	√	√	√	34.3	12.4

[a]Conditions: $Co_{1.11}Te_2 \subset C$ (1 mg), $[Ru(bpy)_3]Cl_2 \cdot 6H_2O$ (5 mg), acetonitrile : H_2O : TEOA = 4 mL : 1 mL : 1.5 mL in the quartz tube of 55 mL, CO_2 (1 atm), irradiation with white LEDs lamp at room temperature. [b]Degassed with argon.

References

1 H. Hu, J. Zhang, B. Guan and X. W. Lou, *Angew. Chem. Int. Ed.*, 2016, **55**, 9514.

2 J. Taylor, M. Brandbyge and K. Stokbro, *Phys. Rev. Lett.*, 2002, **89**, 138301.

3 J. P. Perdew, K. Burke and M. Ernzerhof, *Phys. Rev. Lett.*, 1996, **77**, 3865.

4 G. Kresse and J. Hafner, *J. Phys. Rev. B*, 1993, **47**, 558.

5 G. Kresse and J. Hafner, *J. Phys. Rev. B*, 1994, **49**, 14251.

6 P. E. Blochl, *Phys. Rev. B*, 1994, **50**, 17953.

7 G. Kresse and D. Joubert, *Phys. Rev. B*, 1999, **59**, 1758.